Integrating Surface Modification to Improve the Electrochemical Performances of Li-rich cathode materials

Xiaoyuan Zhang[123]; Yanxiao Gao[123]; Xiangnan Li[123]; Wenfeng Liu[123]; Huishuang Zhang[123]; Shu-ting Yang *[123]; Yanhong Yin *[123]

[1]*School of Physics, School of Chemistry and Chemical Engineering, Henan Normal University, Xinxiang, Henan 453007,*

[2]*National and Local joint Engineering Laboratory of Motive Power and Key Materials, Xinxiang, Henan 453007, China*

[3]*Collaborative Innovation Center of Henan Province for Motive Power and Key Materials, Xinxiang, Henan 453007, China*

Experimental section

Material Characterization

Crystal structure of the cathode materials was characterized by X-ray diffraction (XRD, AXS D8 Advance, Bruker) with Cu Kα radiation for 2θ between 10 and 80° with a step size of 0.02 $°s^{-1}$. Raman analysis was achieved using the Raman spectra equipment (HORIBA, LabRAM HR Evolution) with the 523 nm line of an argon-ion laser. X-ray photoelectron spectroscopy analysis (XPS) was determined by ESCALAB250Xi spectrometer (Thermo Fisher) with monochromatic Al Kα radiation (hν = 1486.6 eV). The particle morphology analysis was conducted with a scanning electron microscope (SEM, SU-8010F, HITACHI). Transmission electron microscope (TEM, HT-7700, Hitachi) with an energy-dispersive Xray spectroscopy (EDS) detector was applied to characterize the detailed structural characterizations and elemental distribution of the samples. The dissolution of Mn and Ni of the cycled electrode to the electrolyte was detected by inductively coupled plasma mass spectrometer (ICP-MS, Perkin Elmer co. Ltd of USA, ELAN DRC-e). In-situ XRD test was carried out to investigate the structural change of LR and LR-2 Li-rich materials during the charge and discharge processes. The differential electrochemical mass spectroscopy (DEMS) measurements were carried out to detect the gas evolution during charging and discharging.

Electrochemical Measurements

All the electrochemical evaluations were performed using coin cells (CR-2025) which were assembled in an insert argon atmosphere. The as-prepared materials, acetylene black and polyvinylidene fluoride binder were mixed with N-methyl-2-pyrrolidine by a mass ratio of 8:1:1. Lithium metal was used as the anode and reference electrode. 1 M $LiPF_6$ (DMC:EC=1:1) was employed as the electrolyte. Galvanostatic charge-discharge experiment data were carried out by CT2001A, Wuhan LAND Cell test system. The batteries were cycled at 0.1 C rate for the first three cycles and then cycled at 0.5 C rate. AC impedance measurements were performed on an electrochemical workstation of CHI660E, Shanghai. The data was obtained in the frequency range from 0.1 to 100 000 Hz with the AC amplitude of 5mV. The galvanostatic intermittent titration (GITT) of the assembled cells was performed using a LAND-CT2001A battery test system between 2.1 and 4.8V at room temperatures.

In-situ XRD observation:

In-situ XRD test was carried out to investigate the structural change of LR and LR-2 Li-rich materials during the charge and discharge processes. A detailed description of in-situ XRD cell for the Li-ion battery was employed. In detail, a thin aluminum window (thickness, 12μm) has been fixed on the cathode case of the cell as a sight window. The cathode was assembled at the bottom of the cell with the active material face upward. 45 μL of electrolyte 1 mol/L $LiPF_6$ in ethylene carbonate/diethyl carbonate (EC/DEC) was homogeneously dropped onto the glassy fiber filter separator (GF/A, Whatman). The current and potential outputs from the potentiostat were recorded by a multifunction data acquisition module/amplifier (PGSTAT30 Differential Electrometer, Autolab), which was controlled by General Purpose Electrochemical Software (GPES). Typically, the galvanostatic control was carried out at a current density of 15 mA/g for initial cycle and the second charge process. Before characterizations, the cell was kept on an open circuit for 4 h.

In-situ DEMS measurements.

In situ DEMS analysis was carried out to detect the gases generated during the initial charge–discharge process. The DEMS cell was assembled in an Ar-filled glove box. In all, the electrolyte was 1 M $LiPF_6$ (DMC:EC=1:1), and the porous polyethylene

film was used as a separator. Electrodes were prepared by casting a slurry with a composition of 80 wt. % active materials, 10 wt. % Super P and 10 wt. % PVDF on to an aluminium current-collector foil. And the typical loading of the active material was 7-8 mg·cm^{-2} on an Al foil. The DEMS measurement was started 3 h before the cell was operated to obtain a stable gas evolution background. The electrochemical measurements were carried out at 0.1C for charge and discharge.

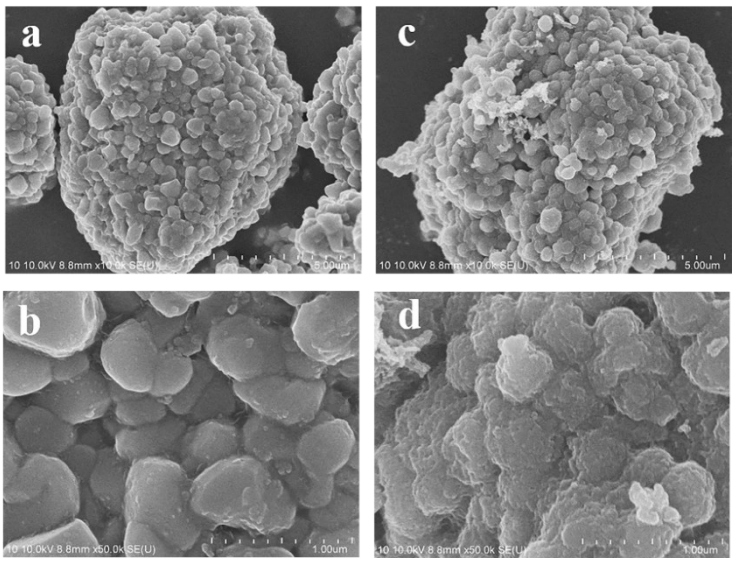

Fig. S1 The SEM images and enlarged region of (a-b) LR-1, (c-d) LR-3

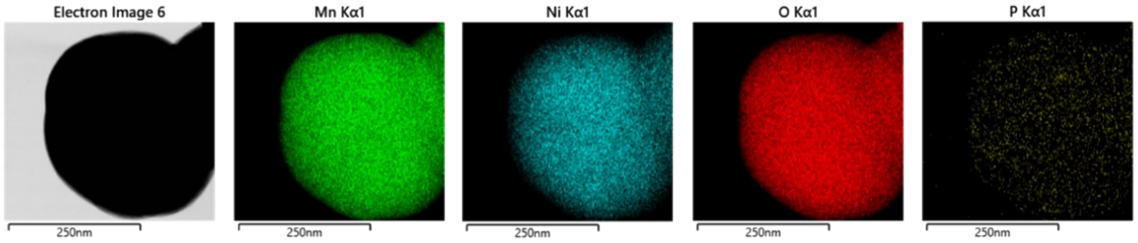

Fig S2 The element mapping of the LR-2.

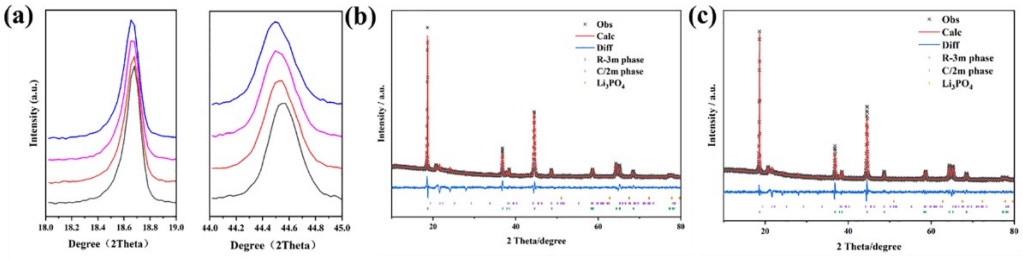

Fig S3 (a) The enlarged image of XRD pattern; The Rietveld refinement results of (b) the LR-1 and (c) the LR-3

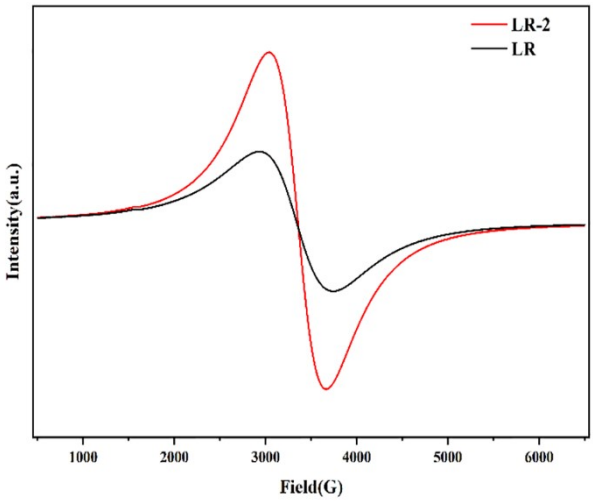

Fig S4 EPR spectra of LR and LR-2

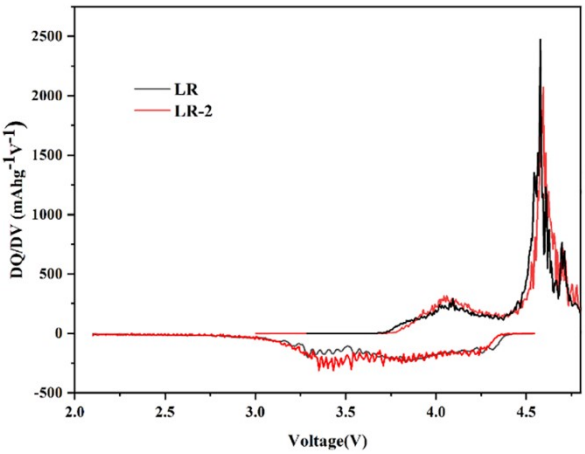

Fig S5 dQ/dV versus V plots for the first cycles of LR and LR-2

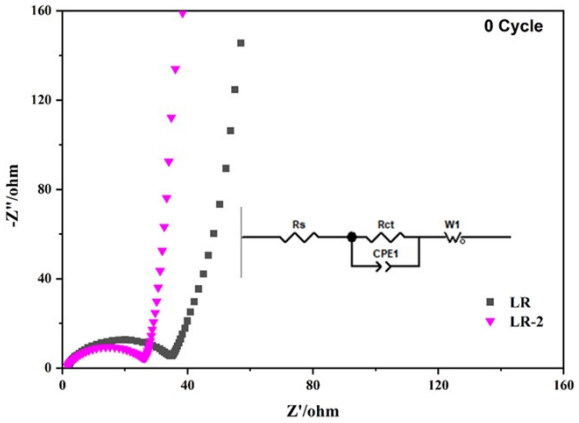

Fig S6 Nyquist plots of LR and LR-2 before cycle (The inserted diagram depicts the equivalent circuit employed for fitting).

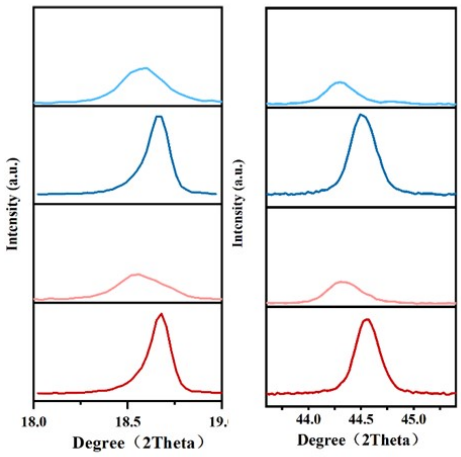

Fig S7. The magnified XRD pattern image.

Supplementary Note 1

The lithium ion diffusion coefficient is an important parameter influencing the rate performance of LIB electrode materials. Therefore, the GITT method was used to determine the lithium ion diffusion coefficient of LR and LR-2. Fig. 5d shows the GITT curves during the first charge/discharge and the comparison of Li ion diffusion coefficients of the two samples, respectively. The value of D_{Li^+} can be calculated by the following formula:

$$D_{Li^+} = \frac{4}{\pi\tau}\left(\frac{m_B V_m}{M_B S}\right)^2\left(\frac{\Delta E_S}{\Delta E_\tau}\right)$$

Where τ is 20 min, ΔE_s and ΔE_τ are obtained from charge-discharge voltage profiles, while m_B is the loading amount of the active substance (g), M_B is the molecular weight of the material (g mol^{-1}), S is the surface area of the electrode (cm^2), and V_m is the molar volume of the material deduced from the crystallographic data (cm^3 mol^{-1}).

Table S1. Lattice parameters obtained from Rietveld refinement of all samples.

sample	a/Å	c/Å	O occupancy	w(Li_3PO_4)%	Rp(%)
LR	2.856344	14.235986	0.9757	0	1.89
LR-1	2.867635	14.258664	0.9654	0.49	1.89
LR-2	2.867838	14.263625	0.9238	0.74	1.82
LR-3	2.867911	14.266721	0.9357	1.60	1.90

Table S2. The fitted parameters of LR and LR-2 before cycles.

	Rs(Ω)	Rct(Ω)
LR	1.739	24.27
LR-2	1.634	21.09

Table S3. The comparison of the capacity retention and discharge median voltage drop of some reported $Li_{1.2}Mn_{0.6}Ni_{0.2}O_2$ (LR) for Li-ion batteries.

Cathode materials	Voltage drop (V)	Capacity retention (%)	Cycle numbers	Current rate	References
LR@Spinel	0.23	97%	100	0.2C	[1]
LR@Spinel@MgF_2	0.45	80%	300	0.5C	[2]
LR@Li_2SiO_3	0.14	86.8%	200	1C	[3]
LR/ Polyanion@ Spinel	0.16	75%	500	1C	[4]
LR@ LiPPA/PPy	0.242	88.5%	100	0.5C	[5]
LR/Vo	0.39	77.2%	200	1C	[6]
Ti/LR	0.365	88.5%	100	1C	[7]
Al/LR	0.349	78.8%	300	0.2C	[8]
LR/Vo@Li_3PO_4	0.11	92.3%	200	0.5C	this work

References

1. Li, Q.; Ning, D.; Zhou, D.; An, K.; Wong, D.; Zhang, L.; Chen, Z.; Schuck, G.; Schulz, C.; Xu, Z.; Schumacher, G.; Liu, X., The effect of oxygen vacancy and spinel phase integration on both anionic and cationic redox in Li-rich cathode materials. *Journal of Materials Chemistry A* **2020,** *8* (16), 7733-7745

2. Zhu, W.; Tai, Z.; Shu, C.; Chong, S.; Guo, S.; Ji, L.; Chen, Y.; Liu, Y., The superior electrochemical performance of a Li-rich layered cathode material with Li-rich spinel Li4Mn5O12 and MgF2 double surface modifications. *Journal of Materials Chemistry A* **2020,** *8* (16), 7991-800

3. Gao, Y.; Liu, W.; Cui, Y.; Zhang, H.; Li, X.; Dong, H.; Yue, H.; Yang, S.; Yin, Y., Silicic Acid-Assisted Interface Engineering Strategy to Improve the Performance of Li1.2Mn0.6Ni0.2O2 Cathode Material. *Acs Appl Energ Mater* **2022,** *5* (10), 12109-12119

4. Chang, Z.; Zhang, Y.; He, W.; Wang, J.; Zheng, H.; Qu, B.; Wang, X.; Xie, Q.; Peng, D.-L., Surface Spinel-Coated and Polyanion-Doped Co-Free Li-Rich Layered Oxide Cathode for High-Performance Lithium-Ion Batteries. *Industrial & Engineering Chemistry Research* **2022**

5. Mu, K.; Tao, Y.; Peng, Z.; Hu, G.; Du, K.; Cao, Y., Surface architecture modification of high capacity Li1.2Ni0.2Mn0.6O2 with synergistic conductive polymers LiPPA and PPy for lithium ion batteries. *Appl Surf Sci* **2019,** *495*

6. Bao, L.; Wei, L.; Fu, N.; Dong, J.; Chen, L.; Su, Y.; Li, N.; Lu, Y.; Li, Y.; Chen, S.; Wu, F., Urea-assisted mixed gas treatment on Li-Rich layered oxide with enhanced electrochemical performance EPR. *Journal of Energy Chemistry* **2022,** *66*, 123-132

7. Liu, S.; Yan, X.; Li, P.; Tian, X.; Li, S.; Tao, Y.; Li, P.; Luo, S., Ti-Doped Co-Free Li1.2Mn0.6Ni0.2O2 Cathode Materials with Enhanced Electrochemical Performance for Lithium-Ion Batteries. *Inorganics* **2024,** *12* (3)

8. Yu, W.; Zhao, L.; Wang, Y.; Huang, H.; Zhang, S.; Li, H.; Liu, X.; Dong, X.; Wu, A.; Li, A., Modulating the local electronic structure via Al substitution to enhance the electrochemical performance of Li-rich Mn-based cathode materials. *Journal of Alloys and Compounds* **2023,** *947*